Steps or Terraces? Dynamics of Aromatic Hydrocarbons Adsorbed at Vicinal Metal Surfaces

Javier Camarillo-Cisneros,[1,3] Wei Liu,[1,2] and Alexandre Tkatchenko[1,*]

[1]*Fritz-Haber-Institut der Max-Planck-Gesellschaft, Faradayweg 4-6, D-14195 Berlin, Germany*
[2]*Nano Structural Materials Center, School of Materials Science and Engineering, Nanjing University of Science and Technology, Nanjing 210094, Jiangsu, China*
[3]*Centro de Investigación en Materiales Avanzados, Miguel de Cervantes 120, C.P. 31109, Chihuahua, Mexico*

The study of how molecules adsorb, diffuse, interact, and desorb from imperfect surfaces is essential for a complete understanding of elementary surface processes under relevant pressure and temperature conditions. Here we use first-principles calculations to study the adsorption of benzene and naphthalene on a vicinal Cu(443) surface with the aim to gain insight into the behavior of aromatic hydrocarbons on realistic surfaces at a finite temperature. Upon strong adsorption at step edges at a low temperature, the molecules then migrate from the step to the (111) terraces, where they can freely diffuse parallel to the step edge. This migration happens at temperatures well below the onset of desorption, suggesting a more complex dynamical picture than previously proposed from temperature-programed desorption studies. The increase of the adsorption strength observed in experiments for Cu(443) when compared to Cu(111) is explained by a stronger long-range van der Waals attraction between the hydrocarbons and the step edges of the Cu(443) surface. Our calculations highlight the need for time-resolved experimental studies to fully understand the dynamics of molecular layers on surfaces.

PACS numbers: 68.43.-h, 68.35.Ja, 68.60.Dv

Microscopic understanding of the thermodynamics and kinetics of organic molecules at inorganic substrates plays an increasingly important role in modern surface science and technology [1–6]. Obviously, the predictive modeling and understanding of the structure, stability, and dynamics of such hybrid systems is an essential prerequisite for tuning their electronic properties and functions [7–10]. In recent years, remarkable progress has been achieved in understanding the structure and stability of molecules on close-packed surfaces by an intensive joint effort between experiment and theory [11]. For some of the well-defined model systems, such as benzene adsorbed on close-packed (111) metal surfaces, state-of-the-art calculations and experiments now often agree to better than 0.1 Å in vertical adsorption heights and 0.1–0.2 eV in adsorption energies [11–13]. However, the functionality of realistic interfaces with applications in catalysis, light-emitting diodes, single-molecule junctions, molecular sensors and switches, and photovoltaics is often determined by interactions of molecules with more complex ("imperfect") substrates [3,14–18]. Therefore, a complete understanding of the dynamics and reactivity of such interfaces demands reliable modeling of the interaction of adsorbed organic molecules with steps, kinks, impurities, and defects. Obviously, the main difficulty here consists of accurately capturing all the relevant energy contributions involved in binding on imperfect substrates, including Pauli repulsion, covalent hybridization, charge transfer, and van der Waals (vdW) attraction. Especially difficult are

cases in which both chemical bonds and vdW interactions make substantial contributions to the overall adsorption process.

In this context, this Letter focuses on modeling and understanding the adsorption, diffusion, and desorption (ADD) mechanisms of fundamental aromatic hydrocarbons—benzene (Bz) and naphthalene (Np)—on the vicinal Cu(443) surface. The temperature-dependent behavior of these systems has been previously studied by temperature-programed desorption (TPD), low-energy electron diffraction (LEED), and scanning tunneling microscopy (STM) [19]. It was concluded that a visible increase in the desorption temperature for Bz on Cu(443) compared to Cu(111) stems from a stronger adsorption along the step edges in the former case. Our calculations provide an alternative three-step mechanism for the dynamics of Bz and Np on the vicinal Cu(443) surface. We find that, upon strong adsorption on step edges at a low temperature, the molecules then migrate from the step to the (111) terraces, where they can freely diffuse parallel to the step edge. This migration happens at temperatures well below the onset of desorption. The increase in the desorption temperature observed in experiments for the Cu(443) surface when compared to Cu(111) is explained by a stronger vdW attraction between the hydrocarbons and the step edges of the Cu(443) surface.

All calculations in this work employ dispersion-inclusive density-functional theory (DFT), specifically using the DFT + vdW^{surf} method [20], combined with the

Perdew-Burke-Ernzerhof (PBE) exchange-correlation functional [21]. The PBE + vdW^{surf} method has already been successfully applied to study the adsorption and reactions of a wide variety of molecules on (111) metal surfaces, often achieving quantitative accuracy for structures and adsorption energies in comparison to state-of-the-art x-ray standing wave, TPD, and microcalorimetry experiments [11,22,23]. In this study, the PBE + vdW^{surf} method is applied to a vicinal surface for the first time, demonstrating that its relative accuracy also extends to adsorption on stepped substrates. Most calculations in this work were carried out using the all-electron code FHI-aims [24]. Transition-state geometries were determined using the CASTEP code [25,26]. See Supplemental Material (Ref. [27]) for more details about our DFT calculations and convergence studies. Our calculations are fully converged in terms of numerical settings, using parameters employed before in our study of Bz adsorption on transition metal surfaces [12,13].

Before proceeding to study the ADD behavior of Bz and Np on Cu(433), we start by systematically analyzing the static potential-energy surface (PES) for these systems. We have carried out extensive geometry optimizations starting from different initial structures, where the Bz and Np molecules are situated in different adsorption sites

and rotated by either 0° or 30° with respect to the [1$\bar{1}$0] direction of the Cu(443) surface. As can be appreciated in Figs. 1(a) and 1(b), there is a clear preference for adsorption of Bz and Np on top of step edges and the appearance of many metastable states near the step edges and on terraces of the Cu(443) surface. This complex situation is in marked contrast with the close-packed Cu(111) surface, where the PES for the adsorbed Bz and Np is essentially flat and their ADD dynamics are well understood [13]. TPD studies of Bz/Cu(111) exhibit a single peak in the desorption spectrum, and STM investigations suggest that the Bz molecules are freely diffusing on the Cu(111) surface at a low temperature [28]. On the Cu(443) surface, the preferred adsorption on step edges can be explained by reactive dangling bonds, and therefore both Bz and Np are able to form weak chemical bonds with the Cu atoms there. In fact, the most stable step-edge adsorption sites for both Bz and Np exhibit adsorption energies that are larger by ∼0.45 eV for Bz and ∼0.60 eV for Np compared to the binding strength on the close-packed Cu(111) surface. The adsorption energies of Bz and Np and the structures of Bz on Cu(443) for several characteristic configurations found in our extensive exploration of the PES are shown in Figs. 1(a)–1(c). The symmetry breaking introduced by step edges leads to a range of adsorption energies on the
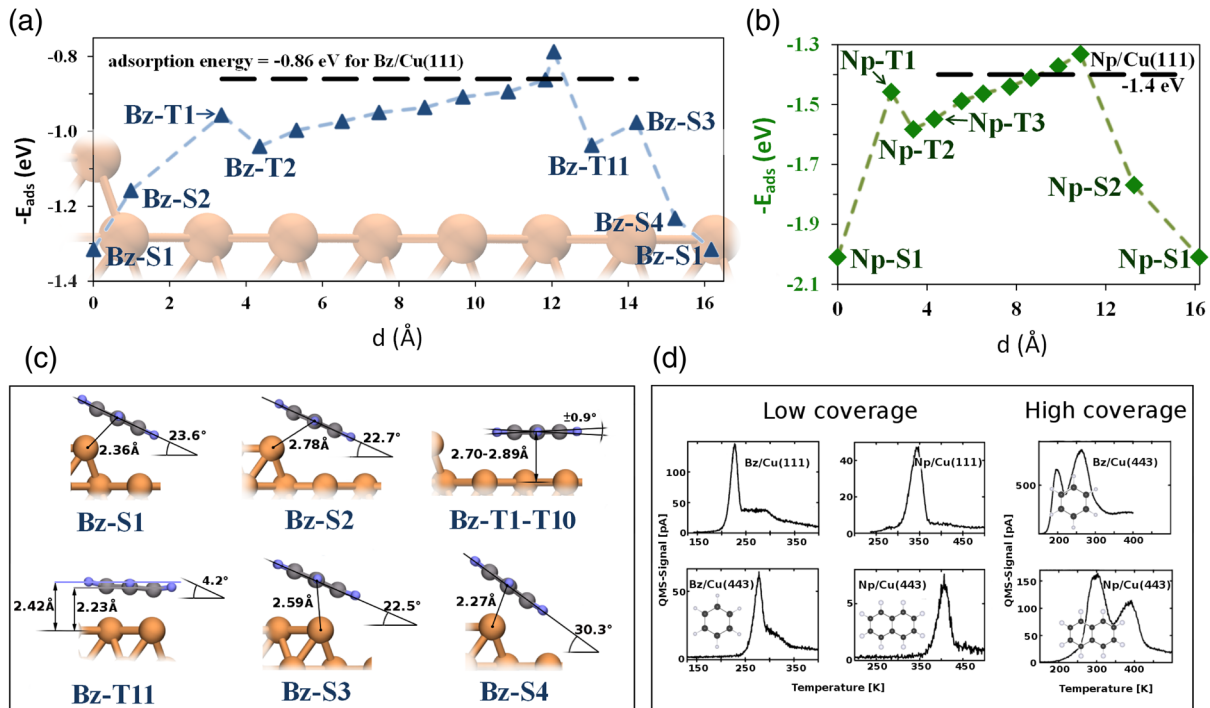

FIG. 1 (color online).   Adsorption energy as a function of distance d measured from the molecule center of mass to the step edge of the Cu(443) surface. Geometries and energies were obtained using the PBE + vdW^{surf} method for (a) benzene/Cu(443) and (b) naphthalene/Cu(443). The letters "S" and "T" denote the "step" and "terrace" of the Cu(443) surface, respectively. Adsorption heights and tilt angles for several Bz/Cu(443) metastable configurations are shown in (c). In (d), we show the TPD spectra for the desorption of Bz and Np from Cu(111) adsorbed at low coverage and Cu(443) adsorbed at low and high coverages. The TPD spectra are adapted from Ref. [19].

Cu(443) terrace: from 0.8 to 1.1 eV for Bz (Bz-$T1$ to Bz-$T11$) and from 1.3 to 1.6 eV for Np (Np-$T1$ to Np-$T9$), where the notation $T1$ to $T11$ denotes the possible adsorption sites for Bz and Np on the terrace (T) of Cu(443); see Fig. 1. The adsorption energies (E_{ads}) on the terrace depend on the distance d from the step edge; in fact, E_{ads} in Figs. 1(a) and 1(b) exhibits a nearly linear behavior with respect to d. This linear dependence can be mainly attributed to the stronger vdW attraction near the step edge, since the pure PBE adsorption energies are essentially degenerate for all configurations of Bz and Np adsorbed on flat terraces. However, also the variation of vertical adsorption heights and local electric fields close and far from the step contribute to the observed quasilinear adsorption energy on the Cu(443) terraces. Although some of the calculated metastable states may correspond to saddle points, this fact does not change any of our conclusions. The values of E_{ads} obtained from PBE + vdW$^{\text{surf}}$ calculations are in the range of adsorption enthalpies estimated from TPD desorption peaks [19,29]. In contrast, pure PBE calculations [21] lead to a flat PES, with adsorption on terraces being endothermic.

The equilibrium height and tilt of Bz are sensitive to the adsorption position. On the terrace the molecules are essentially flat with vertical heights between 2.70 and 2.89 Å, while for the adsorption on step edges Bz tilts from 22° to 30° relative to the terrace and forms covalent bonds to the Cu atoms at the step with C-Cu distances ranging from 2.27 to 2.78 Å from the edge to the molecule center. For Np, the most stable configurations correspond to the long axis of the molecule aligned parallel to the step edge. The adsorption height variation for different metastable states of Np/Cu(443) is much smaller than for Bz/Cu(443), its average value being 2.76 Å.

At this point, it is worthwhile to compare our calculated E_{ads} values with the available experimental estimates obtained from TPD desorption peaks. To determine adsorption enthalpies from TPD desorption temperatures, we utilize the Redhead equation [30], which requires the knowledge of desorption prefactors that depend on the difference between the entropy of the adsorbed molecule and its counterpart in the gas phase. The usual prefactor $\nu = 10^{13} s^{-1}$, derived for desorption of small molecules, was frequently utilized due to the lack of knowledge of precise entropy differences. The situation has been significantly improved after the seminal work of Campbell and Sellers [31,32], who have assembled an extensive data set of ΔS values for adsorbed molecules. We recently used the Campbell-Sellers method to determine a prefactor of $10^{15.2} s^{-1}$ for the desorption of Bz on coinage metal surfaces [13], which we use here for both Bz and Np. In short, the Redhead equation can be written as

$$H_d = k_B T_d \left[\ln \frac{T_d \nu}{\beta} - 3.64 \right], \qquad (1)$$

where T_d is the desorption temperature, k_B is the Boltzmann constant, β is the heating rate, and ν is the preexponential factor. The adsorption enthalpies determined in this way were converted into energies by adding $3k_B T_d / 2$ [13]. Starting with the simplest case of Bz on Cu(111), the PBE + vdW$^{\text{surf}}$ adsorption energy of 0.86 eV is slightly overestimated compared to $E_{\text{ads}} = 0.71$ eV determined from the experimental TPD analysis. Since our main interest is investigating the behavior of molecules on Cu(111) vs Cu(443), this slight overestimation largely cancels out in energy differences as discussed below.

The adsorption of Bz and Np on Cu(443) and Cu(111) surfaces has been thoroughly studied experimentally by Lukas et al. [19]. For adsorption at low coverages, they observed an increase of 50 K in the desorption temperature for Bz/Cu(443) when compared to Bz/Cu(111) [see Fig. 1(d)]. This difference was attributed to the adsorption of Bz on step edges of the Cu(443) surface. Until now, it was not possible to rationalize this observation using first-principles calculations due to recent developments of reliable methods for treating vdW interactions for molecules at surfaces. The increase of the desorption temperature from 228 K for Bz/Cu(111) to 278 K for Bz/Cu(443) corresponds to a difference in adsorption energy of 0.15 eV. This is a factor of 3 smaller than the difference in adsorption energy of 0.45 eV predicted by our calculations, corresponding to adsorption of Bz on step edges of Cu(443) vs terraces on Cu(111). However, such a comparison assumes that the molecules remain in their ground state geometric configuration close to desorption temperatures, thereby ignoring any kinetic effects.

In the case of Np/Cu(443) vs Np/Cu(111), the difference between experiments and our calculations is apparently even larger. TPD experiments observe a desorption temperature of 349 K for Np/Cu(111) and 410 K for Np/Cu(443). This amounts to a difference in adsorption energy of 0.2 eV, compared to 0.6 eV found in our PBE + vdW$^{\text{surf}}$ calculations.

To rationalize this apparently significant discrepancy between TPD experiments and first-principles results, we systematically calculated the migration barriers for diffusion of Bz and Np on the Cu(443) surface for different initial and final metastable states. The energetics of some representative diffusion pathways is shown in Fig. 2. An important observation is that all of the computed barriers are much smaller than the corresponding adsorption energies. This suggests that the adsorbed molecules are likely to be mobile on the Cu(443) terraces already well below desorption temperatures. TPD experiments can only provide information about the molecules upon desorption, given the macroscopic temperature increase rates. Therefore, the TPD spectra do not contain information about the dynamics of adsorbed molecules prior to the desorption process.

The lowest barrier for diffusion from step edges to terraces of the Cu(443) surface determined in our
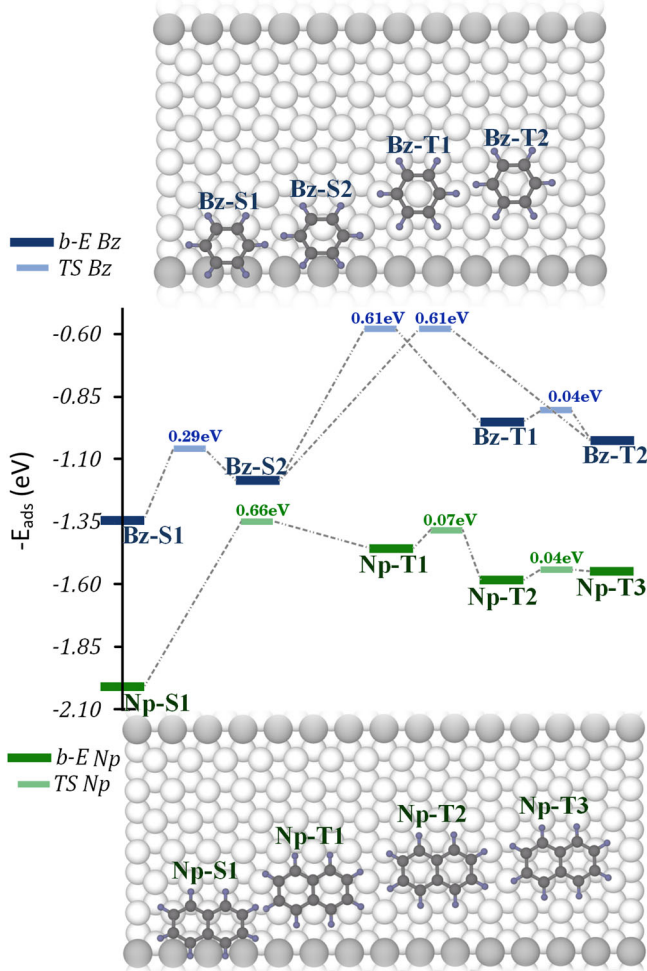
FIG. 2 (color online).   Adsorption energies $(b-E)$ and diffusion barriers (TS) for Bz (upper blue line) and Np (lower green line), determined from PBE + vdW$^{\text{surf}}$ calculations. Structural models are also shown, where all stable configurations correspond to Fig. 1, viewed from the top.

PBE + vdW$^{\text{surf}}$ calculations is 0.61 eV for Bz and 0.66 eV for Np. Using a prefactor of $10^{16}s^{-1}$ in the Arrhenius equation, these barriers would correspond to ∼200 K for Bz/Cu(443) and ∼220 K for Np/Cu(443). Both temperatures are smaller than the desorption temperatures observed in TPD experiments, thereby providing a strong support for our alternative dynamic explanation of the ADD mechanism for Bz and Np on the Cu(443) surface. Another support for our theoretical predictions is the fact that no ordered diffraction pattern could be observed for Np/Cu(443) by LEED at temperatures slightly above 300 K [19]. This strongly suggests that Np molecules freely diffuse on the Cu(443) terraces well below their desorption temperature of 410 K. We note in passing that our conclusions about the migration mechanism would not be modified by changes of the prefactor by 2 orders of magnitude. In addition, we have carried out calculations

using a nonlocal vdW functional optB86b-vdW [33], fully reproducing the PBE + vdW$^{\text{surf}}$ results.

How then can we explain the increase of ∼50 K in desorption temperature observed in TPD for Cu(443) compared to Cu(111)? Since the migration barriers between different metastable states on Cu(443) terraces are significantly below the desorption temperature, we can simply use a Boltzmann average over the energies of all accessible metastable states to calculate the adsorption energy on Cu(443) at a given desorption temperature. Using this procedure, we obtain an increase of 0.16 eV for the adsorption on terraces of Bz/Cu(443) compared to Bz/Cu(111), while for Np/Cu(443) the corresponding increase is 0.19 eV. These values are in excellent agreement with the peaks observed in TPD experiments that lead to an increase of the adsorption energy of 0.15 eV when going from Bz/Cu(111) to Bz/Cu(443) and to an increase of 0.20 eV when going from Np/Cu(111) to Np/Cu(443). This analysis demonstrates that the desorption signal from Cu(443) arises from mobile molecules adsorbed on the terraces of the Cu(443) surface and not from molecules located at step edges.

Finally, we rationalize experimental observations for the adsorption of Bz and Np on Cu(443) for monolayer and higher coverages, where the desorption mechanism is even more complex. In this case, two well-resolved peaks appear in the TPD spectra [see Fig. 1(d)]: for Bz/Cu(443) at 190 and 260 K, while for Np/Cu(443) the peaks are located at 300 and 385 K. The coexistence of two peaks was interpreted as an indication of initial desorption from terraces, followed by the desorption from step edges. It is noticeable that the temperature of the higher desorption peak remains similar as in the case of adsorption on Cu(443) at low coverages, while the lower peak is displaced to decreasing temperatures even when compared to desorption from Cu(111). In experiments, it is evident that both step edges and terraces are populated with Bz and Np molecules upon increasing the surface coverage [19]. Since adsorption on terraces leads to lower stability, these molecules desorb first, explaining the first TPD peak at 190 K for Bz/Cu(443) and 300 K for Np/Cu(443). The low temperatures of these peaks arise from repulsive lateral Bz-Bz (Np-Np) interactions at monolayer and higher coverages. Our extensive calculations for full monolayers and double layers (with up to six molecules per 4×1 unit cell for Bz and 6×1 unit cell for Np) yield adsorption energies for the "weakest" molecules of 0.65 ± 0.1 eV for Bz and 0.96 ± 0.1 eV for Np. These values agree particularly well with the adsorption energies of 0.59 eV ($T_d = 190$ K) for Bz and 0.94 eV ($T_d = 300$ K) for Np, determined using Eq. (1) from experimental low-temperature desorption peaks. Once some of the terrace molecules desorb, the temperature is already sufficiently high for the molecules on the step edges to overcome the migration barrier and diffuse into the terraces. We note that

this process can be rather cooperative, as suggested by the very broad nature of the high temperature peak in TPD experiments for high-coverage Bz and Np layers on Cu(443), as shown in Fig. 1(d) [19]. Upon migration of the "former step-edge" molecules onto Cu(443) terraces, the lateral repulsion is now reduced, leading to a higher adsorption strength compared to monolayer coverage and explaining the high-temperature peaks observed in TPD experiments for both Bz and Np. Our analysis also explains why high-temperature or high-coverage peaks arise at temperatures similar to desorption at low coverages. Once the former step-edge molecules have diffused onto Cu(443) terraces, their adsorption energy becomes identical to the scenario where the molecules are adsorbed at low coverage.

In conclusion, we have studied the adsorption, diffusion, and desorption behavior of benzene and naphthalene molecules on the vicinal Cu(443) surface. Our calculations suggest a more complex dynamical picture than previously proposed from temperature-programed desorption studies of these systems. In general, our findings imply that the understanding of molecular adsorption at realistic surfaces at finite temperatures requires a consideration of dynamical effects. This strongly advocates the need for time-resolved experimental studies to understand the behavior of molecular layers on realistic surfaces.

---

[*] tkatchenko@fhi-berlin.mpg.de

[1] N. Koch, N. Ueno, and A. T. S. Wee, *The Molecule-Metal Interface* (Wiley, New York, 2013).

[2] L. Zoppi, L. Martin-Samos, and K. K. Baldridge, Acc. Chem. Res. **47**, 3310 (2014).

[3] K. Golibrzuch, P. R. Shirhatti, J. Geweke, J. Werdecker, A. Kandratsenka, D. J. Auerbach, A. M. Wodtke, and C. Bartels, J. Am. Chem. Soc. **137**, 1465 (2015).

[4] E. Goiri, M. Matena, A. El-Sayed, J. Lobo-Checa, P. Borghetti, C. Rogero, B. Detlefs, J. Duvernay, J. Ortega, and D. de Oteyza, Phys. Rev. Lett. **112**, 117602 (2014).

[5] T. K. Haxton, H. Zhou, I. Tamblyn, D. Eom, Z. Hu, J. B. Neaton, T. F. Heinz, and S. Whitelam, Phys. Rev. Lett. **111**, 265701 (2013).

[6] K. Forster-Tonigold, X. Stammer, C. Wöll, and A. Groß, Phys. Rev. Lett. **111**, 086102 (2013).

[7] F. S. Tautz, Prog. Surf. Sci. **82**, 479 (2007).

[8] L. Kronik and N. Koch, MRS Bull. **35**, 417 (2010).

[9] T. Roman and A. Groß, Phys. Rev. Lett. **110**, 156804 (2013).

[10] J. K. Nørskov, F. Abild-Pedersen, F. Studt, and T. Bligaard, Proc. Natl. Acad. Sci. U.S.A. **108**, 937 (2011).

[11] W. Liu, A. Tkatchenko, and M. Scheffler, Acc. Chem. Res. **47**, 3369 (2014).

[12] W. Liu, J. Carrasco, B. Santra, A. Michaelides, M. Scheffler, and A. Tkatchenko, Phys. Rev. B **86**, 245405 (2012).

[13] W. Liu, V. G. Ruiz, G.-X. Zhang, B. Santra, X. Ren, M. Scheffler, and A. Tkatchenko, New J. Phys. **15**, 053046 (2013).

[14] L. Bartels, Nat. Chem. **2**, 87 (2010).

[15] C. Sanchez, P. Belleville, M. Popall, and L. Nicole, Chem. Soc. Rev. **40**, 696 (2011).

[16] J. D. Horvath, A. Koritnik, P. Kamakoti, D. S. Sholl, and A. J. Gellman, J. Am. Chem. Soc. **126**, 14988 (2004).

[17] R. Zhang *et al.*, Phys. Chem. Chem. Phys. **15**, 20662 (2013).

[18] S. González, F. Viñes, J. F. García, Y. Erazo, and F. Illas, Surf. Sci. **625**, 64 (2014).

[19] S. Lukas, S. Vollmer, G. Witte, and C. Wöll, J. Chem. Phys. **114**, 10123 (2001).

[20] V. G. Ruiz, W. Liu, E. Zojer, M. Scheffler, and A. Tkatchenko, Phys. Rev. Lett. **108**, 146103 (2012).

[21] J. Perdew, K. Burke, and M. Ernzerhof, Phys. Rev. Lett. **77**, 3865 (1996).

[22] W. A. Al-Saidi, H. Feng, and K. A. Fichthorn, Nano Lett. **12**, 997 (2012).

[23] C. Wagner, N. Fournier, F. S. Tautz, and R. Temirov, Phys. Rev. Lett. **109**, 076102 (2012).

[24] V. Blum, R. Gehrke, F. Hanke, P. Havu, V. Havu, X. Ren, K. Reuter, and M. Scheffler, Comput. Phys. Commun. **180**, 2175 (2009).

[25] N. Govind, M. Petersen, G. Fitzgerald, D. King-Smith, and J. Andzelm, Comput. Mater. Sci. **28**, 250 (2003).

[26] S. J. Clark, M. D. Segall, C. J. Pickard, P. J. Hasnip, M. I. Probert, K. Refson, and M. C. Payne, Z. Kristallogr. **220**, 567 (2005).

[27] See Supplemental Material at http://link.aps.org/supplemental/10.1103/PhysRevLett.115.086101 for more details regarding calculations and analysis.

[28] S. Stranick, M. Kamna, and P. Weiss, Surf. Sci. **338**, 41 (1995).

[29] M. Xi, M. Yang, S. Jo, B. Bent, and P. Stevens, J. Chem. Phys. **101**, 9122 (1994).

[30] P. A. Redhead, Vacuum **12**, 203 (1962).

[31] C. T. Campbell and J. R. V. Sellers, J. Am. Chem. Soc. **134**, 18109 (2012).

[32] C. T. Campbell and J. R. V. Sellers, Chem. Rev. **113**, 4106 (2013).

[33] J. Klimeš, D. R. Bowler, and A. Michaelides, J. Phys. Condens. Matter **22**, 022201 (2010).